Paper Number 2005-01-2833

Nuclear Radiation Fields on the Mars Surface: Risk Analysis for Long-term Living Environment

Brooke M. Anderson, Martha S. Clowdsley, Garry D. Qualls
NASA Langley Research Center, Hampton, VA, USA

John E. Nealy
Old Dominion University, Norfolk, VA, USA

ABSTRACT

Mars, our nearest planet outward from the sun, has been targeted for several decades as a prospective site for expanded human habitation. Background space radiation exposures on Mars are expected to be orders of magnitude higher than on Earth. Recent risk analysis procedures based on detailed dosimetric techniques applicable to sensitive human organs have been developed along with experimental data regarding cell mutation rates resulting from exposures to a broad range of particle types and energy spectra. In this context, simulated exposure and subsequent risk for humans in residence on Mars are examined. A conceptual habitat structure, CAD-modeled with duly considered inherent shielding properties, has been implemented. Body self-shielding is evaluated using NASA standard computerized male and female models. The background environment is taken to consist not only of exposure from incident cosmic ray ions and their secondaries, but also include the contribution from secondary neutron fields produced in the tenuous atmosphere and the underlying regolith.

INTRODUCTION

History has recorded that the urge to explore is undeniably a part of the human psyche. The exploits of Columbus, Cook, Gagarin, Armstrong, and many others bear out this fact. The planet Mars is accessible at the present time, and implementation of a short-duration mission only needs sufficient public support and provision of necessary resources. The journey to Mars is projected to take ~ ½ year, and an initial visit may be a short-stay (or "sprint") mission. In the present study, we address the case of a semi-permanent habitat, or outpost, set in place to accommodate a long-duration stay (~1½ to 2 years). Many technical problems must be addressed in the case of the short-duration mission, but additional challenges arise for the long-stay mission, not the least of which is the problem of space radiation exposure.

The evaluation of hazards due to space radiation exposures and assigning acceptable risk limitations continues to be problematic and remains an area of critical research. Exposure limits have been established on the basis of conventional dosimetry for astronauts in Low Earth Orbit (LEO) operations (e. g. Space Shuttle, International Space Station) but remain undefined for deep space missions. Current thinking seems to favor use of the LEO limits as guidelines for deep space mission exposures, principally because computation of conventional exposures based on linear energy transfer (LET) in a target medium by flux of ionizing radiation may be performed with little ambiguity. However, the basis for radiation damage to mammalian cellular systems by continuous low dose rate heavy-ion radiation (galactic cosmic rays – GCR) is related to LET in an indirect and complex fashion. For a given ionizing particle species and energy, cell damage may be highly variable for different cell types.

In the present work, the purpose is to describe some characteristics of long-term GCR exposure for astronauts resident on Mars from the standpoint of conventional dosimetry as well as for initiation of cell transformation in several radiosensitive cell types. Data from radiological experiments have been used to define parameters for the modeling of various cell-damage cross sections. Much of the data for radiation effects is derived from experiments on animals, and it is recognized that damage to laboratory animal cells cannot be equated to human cell damage even for similar cell types and can, at best, serve as indicators of possible effects. Nevertheless, it is felt that animal experiments will continue to be increasingly valuable, particularly with the very great advances being made in genetic biosciences, expanded computation capabilities, and sub-microscopic visualization techniques. It is thus conceivable that viable extrapolation of radiation effects

on animal mammalian cells to their human counterparts may be accomplished in the future with a high degree of confidence.

LONG-STAY MARS HABITAT SCENARIO

The landed module (figures 1 and 2) is designed to be a habitat and a science laboratory for a crew of four at the planetary surface[1]. It was designed to provide crew accommodations and lab support for surface missions, along with providing airlocks for crew EVA and radiation protection. The habitat is capable of autonomous landing and system startup following the landing. It also provides support to the unpressurized rovers and survival power to dormant landers. The facility consists of three levels with a total pressurized volume of 240 m^3; it has an outer diameter of 6.5 meters and an inner diameter 6.0 meters. The lowest level houses two two-person airlocks, which can also act as shelters during solar particle events. It also contains an unpressurized porch that crewmembers may use to dust off prior to vehicle ingress. The second deck contains the science laboratory and the mechanical and avionics systems. The third floor houses the crew quarters, galley and wardroom. The core structure consists of the pressure vessel and aft skirt along with Micro-Meteoroid Object Debris (MMOD) that also serves as the primary structure and integral shroud during launch. The core structure is designed to be a cylindrical pressure vessel at 70. 33-kPa internal pressure and is approximately 6 meters tall by 6 meters in diameter. It was designed to have a 5-year lifetime.

For this study we chose to look at a single point within the crew quarters, as that is where they will most likely spend most of their time. Where the average thickness of material is approximately 4 gm/cm^3, as seen in figure 4.

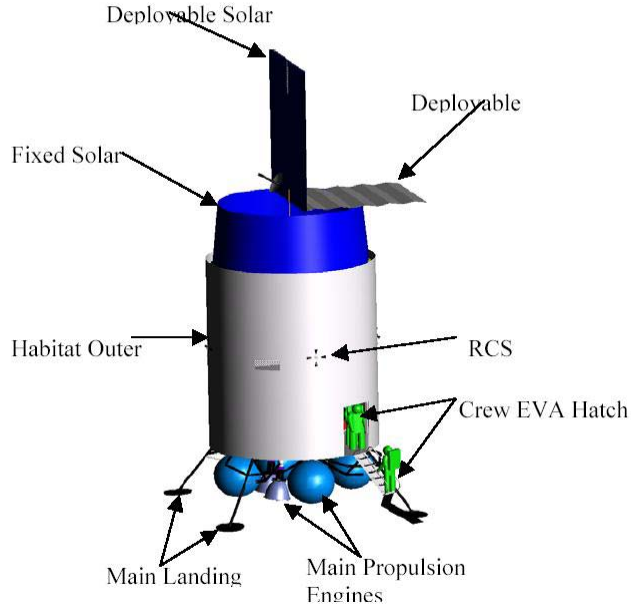


Fig 1. Exterior of Habitat

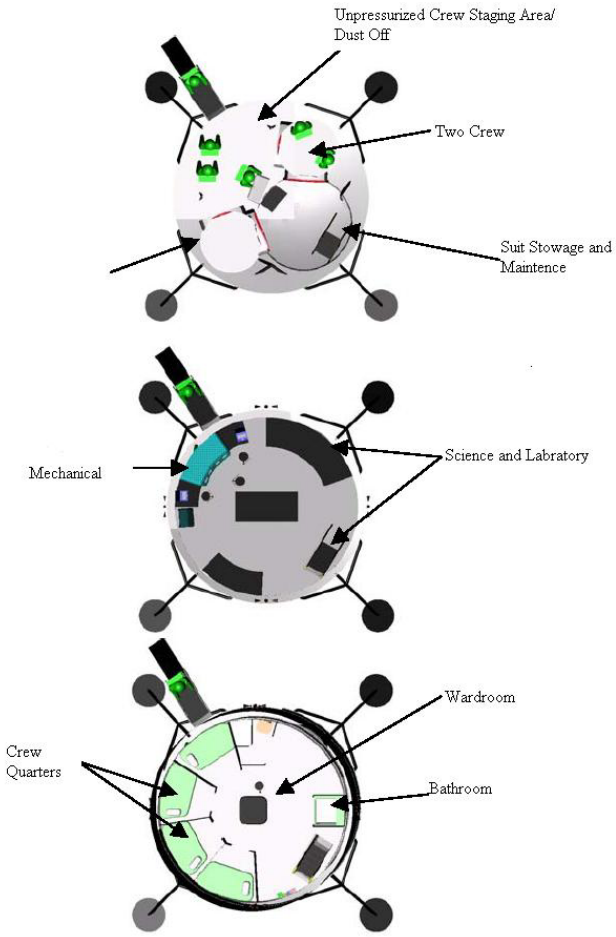


Fig 2. Interior of Habitat

ENVIRONMENT AND TRANSPORT

For the present scenario, the radiation field on Mars is ultimately derived from the interplanetary GCR environment. The NASA Reference Model of Badhwar and O'Neill[2] that includes ion flux for particles of charge 1 through 28 has been implemented. The particle flux generally correlates with observed cosmic elemental abundance, and Figure 3 shows the differential flux vs. energy for some of the more important GCR ions. The GCR-initiated flux field at the planetary surface depends on the thickness of atmosphere traversed. A pure CO_2 atmosphere is assumed for Mars with ambient overhead column amounts of 7 and 15 g/cm^2. The lower value represents a habitat site at high elevation, and the higher value simulates a correspondingly lower altitude.

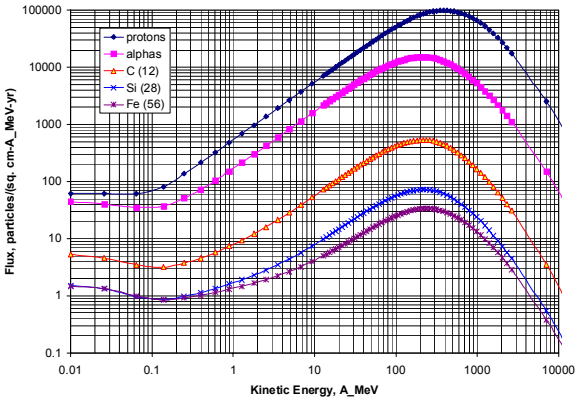


Fig. 3. Free-space GCR flux at solar minimum for selected ions.

The HZETRN code[3] used to compute the GCR transport is a versatile and efficient deterministic program that solves the set of coupled linear Boltzmann transport equations for fluences $\phi_j(\mathbf{x},\mathbf{\Omega},E)$ of type-j particles of energy E at location **x**:

$$\vec{\Omega} \bullet \nabla \phi_j(\vec{x},\vec{\Omega},E) + \sigma_j(E)\phi_j(\vec{x},\vec{\Omega},E) = \sum \int \sigma_{j,k}(\vec{\Omega},\vec{\Omega}',E,E')\phi_k(\vec{x},\vec{\Omega}',E')d\vec{\Omega}'dE'$$

where σ_j and σ_{jk} are macroscopic cross sections in the target medium. The σ_{jk} represent processes for which type k particles moving in direction $\mathbf{\Omega}'$ with energy E′ produce a type j particle in direction $\mathbf{\Omega}$ with energy E (including decay processes). A continuous slowing down process is assumed for charged particle energy loss, with σ_{jk} forward components determined by marching procedures, and isotropic neutron components evaluated with multigroup methods.

The transport calculations have been made assuming three primary material media: the CO_2 atmosphere, the habitat + human body combination, and the underlying regolith. The assumption is also made that the habitat consists primarily of unspecified lightweight materials of high hydrogen content. Transport calculations for a few such materials have been made[4] and have been shown to exhibit GCR attenuation properties similar to H_2O. Thus, the simplifying assumption is made that transport along a given ray direction consists first of the CO_2 slant path through the atmosphere followed by an appropriate H_2O amount representing the effective habitat wall plus body tissue thickness. The third material layer is that of the Martian regolith for which transport of the primary GCR field is performed for a thickness amount of 100 g/cm^2. This final part of the transport calculation defines the flux of back-scattered neutrons near the surface, which contributes to the ultimate exposure at a specified body target point. The regolith composition in terms of atomic mass fraction is taken as[5]:

Table I. Mars Regolith Composition

O^{16}: 0.6246	Fe^{56}: 0.0487	Na^{23}: 0.0187
Si^{28}: 0.1708	Mg^{24}: 0.0360	S^{32}: 0.0159
Al^{27}: 0.0550	Ca^{40}: 0.0273	Cd^{48}: 0.0029

Both habitat and human body involve rather complex spatial geometry; the CAD-modeled habitat has been described previously. For the human geometry, the NASA Computerized Anatomical Male[6] (CAM) and the Computerized Anatomical Female[7] (CAF) have been implemented. The CAF model was derived from the earlier CAM by overall size reduction of 8%, deletion of specifically male organs, and appropriate addition of female organs (breasts, uterus, ovaries). A special algorithm has been used to map the directional distribution of amount of material about selected target points in the CAM and CAF models. The coordinate system used has origin at the top of the head with positive z toward the feet, positive x outward from the chest, and positive y through the right shoulder. The directional grid is based on spherical coordinates consisting of 44 evenly spaced azimuth angles and 22 polar angles chosen so that interstitial solid angles are equal. Six body points have been selected for analysis: three from the CAM model are for a skin point on the thigh, an ocular lens point, and an internal point in the pelvic region representing a blood-forming organ (BFO), along with three specifically female organ target points at the ovary, uterus, and breast locations. The thickness amounts for each target point have been arranged in ascending order and normalized to form cumulative thickness distributions and are shown in Figure 4, along with the thickness distribution for the selected interior point in the habitat.

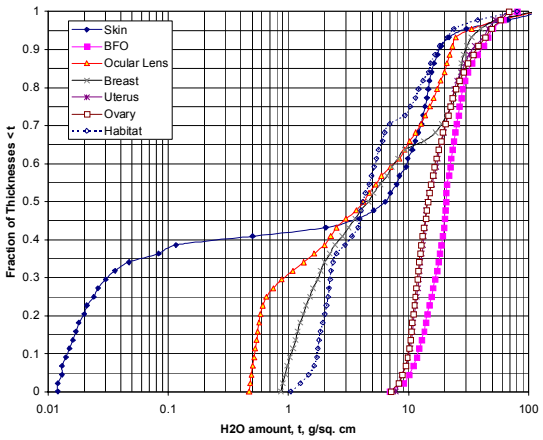


Fig. 4. Cumulative thickness distributions for habitat target point and body target points used in present analysis.

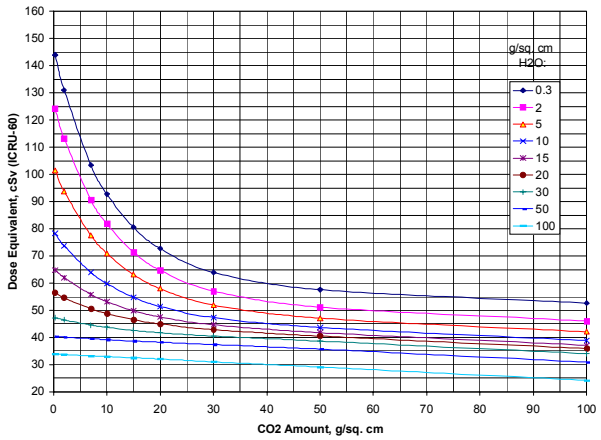


Fig. 5. Results of dose equivalent calculations for combinations of CO_2 and H_2O thickness amounts.

COMPUTATIONAL PROCEDURES

After the differential flux, $\phi_j(\mathbf{x},\mathbf{\Omega},E)$, is determined from the transport calculations, integration over the solid angle gives the corresponding omni-flux, $\Phi(\mathbf{x},E)$, at location **x** which is used in computing the energy deposition, or dose. The dose equivalent, H, for humans must include a quality factor, Q, that relates biological damage from high-energy charged particles to that of gamma rays having equal energy deposition. The quality factors for heavy charged particles are generally substantially greater than unity. Those used in the present analysis are as recommended by the International Commission on Radiation Measurement and Units[8] (ICRU). The dose equivalent is then computed as:

$$H(\vec{x}) = \sum_j \int_0^\infty \Phi_j(\vec{x},E) S_j(E) Q_j(E) dE$$

where S_j is the particle stopping power (dE/dx) in the target material. Dose equivalent values have been evaluated for a matrix of CO_2 + H_2O thickness amounts in units of cSv (rem), and results are presented in Figure 5. The results include contributions from neutrons backscattered from the Mars regolith. Some diagnostic calculations were made without regolith backscatter and indicated that this contribution was about 8% of the total H value.

The effects of high energy radiation on cellular material is not as straightforward, and have been estimated in this study by a 4-parameter cell damage model for both low and high linear energy transfer (LET) particles. The primary background reference for model details and cell survival parameters is that of Katz, et al.[9] The mathematical foundation for the track structure model is given in detail in Cucinotta et al.[10] and Katz et al.[11]

For the low-LET radiation, a multi-target model is used in which two parameters suffice to describe the probability that for a given exposure a cell will be inactivated (killed). These are the "e-folding" dose, D_0, and the number of targets, m, within the cell that must be hit before inactivation can occur. The survival probability for low-LET exposure is then given as

$$\Pi_{Lo} = 1 - [1 - \exp(D_\gamma / D_0)]^m$$

where D_γ is the dose (energy deposition) of the low-LET radiation.

The determination of high-LET effects becomes substantially more complicated, since ejected electrons ("δ-rays") form a radial pattern about the axis of the track that depends on the charge and local energy of the ion. An "action cross section", σ, is defined for an ion interaction with a given cell type, and is calculated for two regimes: (1) when δ-ray interactions occur predominantly within the physical domain of the cell, and (2) when the interactions extend beyond the nominal cell radius. In the first case, the action cross section is calculated as

$$\sigma = \sigma_0 [1 - \exp(-Z^{*2} / \kappa\beta^2]^m$$

where Z^* is an "effective" projectile ion charge and β is the ratio of particle speed to that of light, and is given by

$$Z^* = Z[1 - \exp(-125\beta / Z^{2/3})]$$

and κ is related to an effective sensitive site radius, a_0, as

$$\kappa \propto D_0 a_0^{\,2}$$

with the proportionality constant dependent on units employed and geometric shape of the target cell. When $\sigma/\sigma_0 > 0.95$, an average dose, D_{av}, for energy deposition

in a target of radius a_0 at a distance, t, from the particle track is used to evaluate the action cross section:

$$\sigma = \int_0^\infty 2\pi \{1 - \exp[-D_{av}(a_0, t)/D_0]\} t dt$$

The evaluation of D_{av} then depends on the target dimension a_0 as well as the energy spectrum of emitted δ-rays along the particle track. Again, Katz, et al.[9] presents the formulation in greater detail, and further informative insight on the procedure may be found in a paper by Goodhead[12].

When the value of σ has been computed, the probability of survival after high-LET exposure is simply

$$\Pi_{Hi} = \exp(-\sigma F)$$

where F is the fluence of a particular ion. Finally, the combined fraction of survivors for an initial population N_0 is

$$N / N_0 = (\Pi_{Lo})(\Pi_{Hi})$$

Three radiosensitive mammalian cell types for which the model parameters are available have been chosen for analysis in this study. The action cross section for DNA double strand break is also included for comparison. The subject model parameters have been taken from the more extensive tabular values in Katz, et al.[9] and are:

Table II. Katz Model Cell Parameters

	m	κ	D_0, Gy	σ_0, cm^2
C3H10T1/2 Transformation	3	475	117	7.0E-11
DNA Double Strand Break	1	700	300	1.0E-10
Skin Fibroblast Mutation	3	700	1000	7.0E-11
Harderian Gland Mutation	3	480	225	3.5E-10

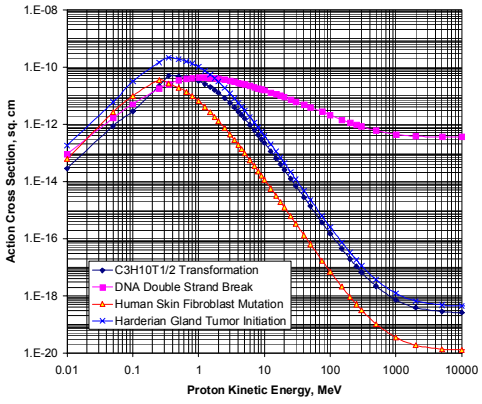


Fig. 6. Energy-dependent cross sections for cell mutations used in analysis.

The energy-dependent cross sections for the transformation processes are shown in Figure 6 for protons. It is seen that the very large decrease in cross section values at higher energies for the cell transformations is not seen for the DNA DSB, and is indicative that the DSB is more likely to occur at the high energies; at low energies, the values are comparable.

For the exposures resulting from GCR on the Mars surface, calculations of cell mutations have been made in a similar manner as that for the dose equivalent, where instead of the dosimetric quantity the mutation probabilities are calculated in accordance with the Katz model. These results are expressed in terms of cells affected per million. Plots of these results are shown in Figures 7, 8, 9, and 10 for the respective cell entities.

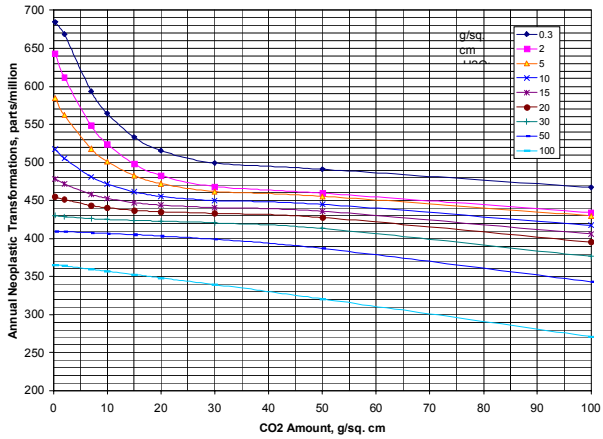


Fig. 7. C3H10T1/2 cell transformation rate for combinations of CO_2 and H_2O thickness amounts.

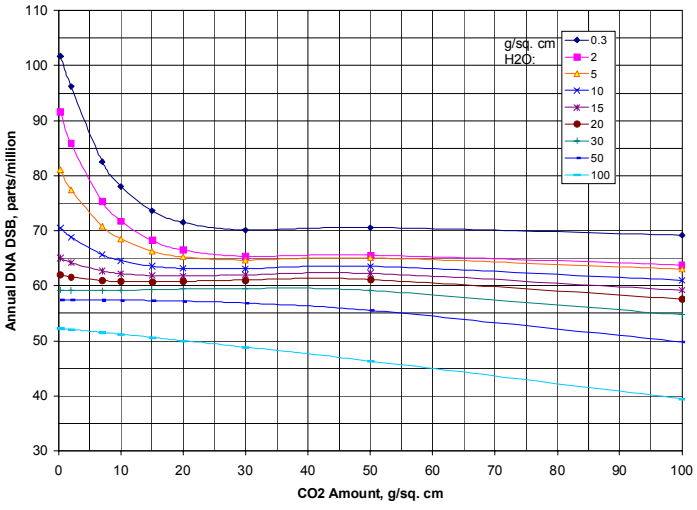


Fig. 8. Rate of DNA Double Strand Break for combinations of CO_2 and H_2O thickness amounts.

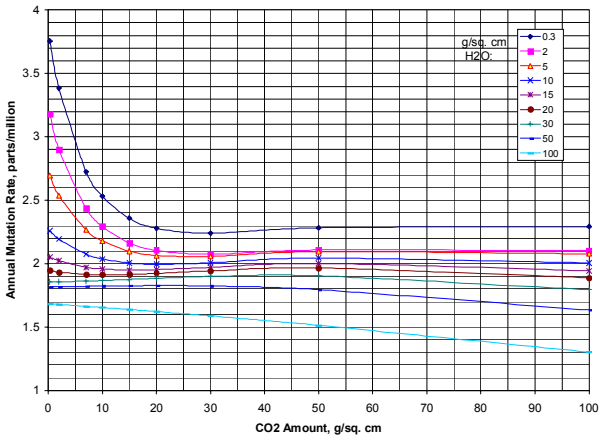


Fig. 9. Rate of human skin fibroblast mutations for combinations of CO_2 and H_2O thickness amounts.

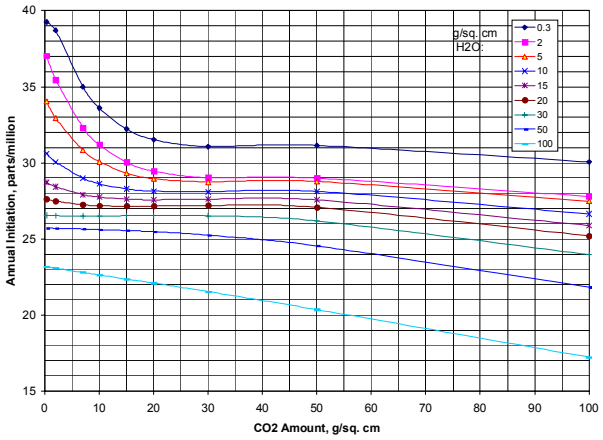


Fig. 10. Harderian gland tumor initiation rate for combinations of CO_2 and H_2O thickness amounts.

It is obvious that the mouse embryo cells (C3H10T1/2) are far more radiosensitive than are the others considered, and the skin fibroblasts are considerably more radiation resistant.

RESULTS OF CALCULATIONS

The results of the transport calculations used in conjunction with the directional thickness distributions of the atmosphere- habitat- human body combination leads to the evaluation of dose equivalent at a specified target point. This procedure has been implemented for an interior crew quarters location in the habitat for the six selected body target points defined previously. The results are shown in Table III for the high and low altitude habitat locations. It should be noted that the GCR flux incident at the top of the atmosphere occupies only ½ of the total sphere of solid angles, and this feature of "planetary shielding" is taken into account for the exposure determinations.

The results do not show a great range for the various body point exposures, even for the high and low altitudes. The most exposed points are obviously the skin, ocular lens, and female breast; the most protected target point is that of the BFO. The female uterus and ovary points are also relatively well protected as can be seen from the thickness distributions of Figure 2.

Table III. Annual Dose Equivalent for Mars Scenario

Target Point	Dose Equivalent, cSv (7 g/cm^2 atmosphere)	Dose Equivalent, cSv (15 g/cm^2 atmosphere)
SKIN	26.4	23.0
LENS	27.4	23.7
BFO	21.2	19.6
BREAST	27.7	23.9
UTERUS	22.6	20.6
OVARY	22.6	20.6

The exposure guidelines derived from the LEO astronaut limits that are most pertinent for the Mars scenario are those for BFO exposure - < 50 cSv annually and < 200 cSv career (BFO career limit for females is 140 cSv). For a stay of up to three years on Mars, the BFO calculations indicate that GCR exposures remain well below their limit guidelines. It must be noted that the present analysis does not consider contributions from solar proton events or those incurred during transit in order to avoid the complicating factors of vehicle configuration, trajectory options, and flare shelters. These aspects may be examined in separate studies. The scenario presented here conservatively assumes a low-density atmosphere and a habitat that provides only inherent shielding from its basic structure (i. e., the pressurized habitat is designed only to provide a "shirt-sleeve" atmosphere).

Although conventional dosimetry analysis may predict acceptable BFO exposures, incurred dose for other radiosensitive organs must bear closer scrutiny, especially the exclusively female organs that are considered here. Along these lines, the cell mutation calculations using the Katz model are examined. Exposures for each of the cell types considered are calculated for two body target points that differ in degree of body self-shielding – the skin and ovary locations. The results are presented in Table IV as annual number of cell transformations per million original cell population.

Table IV. Annual Cell Transformations per million

	7 g/cm^2 atmosphere		15 g/cm^2 atmosphere	
Cell type	Cell @ Skin Location	Cell @ Ovary Location	Cell @ Skin Location	Cell @ Ovary Location
C3H10T1/2	225	215	217	209
DNA DSB	32	30	31	30
Skin Fibroblast	1	1	1	1
Harderian Gland	14	13	14	13

Although it is tempting to try to infer human exposure risk from the cell mutation data, we refrain from doing so here. However, it is believed that some, as yet unknown, relationships do exist and that future research may define them. Nevertheless, some noteworthy features are apparent in the results. For example, it is not surprising that skin fibroblast cells are more radiation tolerant than the others. The very high sensitivity of the C3H10T1/2 (mouse embryo) cells is also notably prominent. Another interesting result is that the rate of DNA double strand breaks is approximately twice that of Harderian gland tumor initiation, but only about 1/7 the rate of embryonic cell transformation.

CONCLUDING REMARKS

The long-duration Mars surface mission considered here has been analyzed from the standpoint of human exposure incurred during the stay from GCR-initiated radiation fields within a habitat having no special dedicated radiation shield mass. Dose contributions from other sources have not been included in the study; exposure from some additional sources may be more readily controlled (e. g. solar protons, fission power reactors) or added after additional analysis (GCR exposure during transit). Exposure guidelines based on limits established for LEO operations have been based on statistical data and quantified so that no more than a 3% increase in contraction of fatal cancer occurs as a result of space radiation exposure. The calculations indicate that for a three-year surface stay, the incurred dose equivalent for the critical BFO exposure is approximately ½ the limit guideline value. Thus, on the basis of conventional dosimetry, one may infer that the radiation risk from GCR would be acceptable for day-to-day mission operations.

The accompanying calculations of cell mutation rates cannot, at present, be used to infer quantified risk for reasons stated in the main text. There are, however, marked similarities in the behavior of the various cell mutation rates as a function of effective shield amount when compared to the conventional dose equivalent behavior. The calculations indicate that the GCR contribution is not readily controlled; after 20 – 40 g/cm^2 effective shielding, the ultra-high energy particles are very penetrating and effects vary slowly with addition of substantial shield amounts. The results for the very high mutation rates of the mouse embryo cells are especially intriguing: ~0.02% cell mutations per million annually. If one speculates that human embryonic cells exhibit similar sensitivity, the implication follows that the act of human procreation on Mars is ill advised. Reduction of GCR-produced radiations to near terrestrial levels would require massive shielding; subterranean habitation quarters may offer one possibility.

Much work remains to be done in this area. The evolution of viable cell kinetic models coupled with continued laboratory research devoted to radiation exposure effects on cell structures may eventually provide the knowledge required to live permanently and safely in a planetary environment. In the course of such research, it is conceivable that new findings with regard to human cell behavior in special circumstances may lead to phenomenal medical advances that could result in the greatest "spin-off" yet resulting from dedicated space exploration activities.

REFERENCES

1. Cook, D., et al., "L1 Lunar Habitat Lander Element Conceptual Design Report," Engineering Directorate, December 2000.
2. Badhwar, G. D. and O'Neill, P. M.: "Improved Model of Galactic Cosmic Radiation for Space Exploration Missions". Nucl. Tracks and Rad. Meas., **16**, no. 3, pp. 403-410, 1992.
3. Wilson, J. W.; Badavi, F. F.; Cucinotta, F. A.; Shinn, J. L.; Badhwar, G. D.; Silberberg, R.; Tsao, C. H.; Townsend, L. W.; and Tripathi, R. K.: "HZETRN: Description of a Free-Space Ion and Nucleon Transport and Shielding Computer Program". NASA TP-3495, 1995.
4. Kim, M. Y.; Wilson, J. W.; Thibeault, S. A.; Nealy, J. E.; Badavi, F. F.; and Kiefer, R. L.: "Performance Study of Galactic Cosmic Ray Shield Materials". NASA TP-3473, 1994.
5. Kim, M. Y.; Thibeault, S. A.; Simonsen, L. C.; and Wilson, J. W.: "Comparison of Martian Meteorites and Martian Regolith as Shield Materials for Galactic Cosmic Rays". NASA TP-1998-208724, 1998.
6. Billings, M. P. and Yucker, W. R.: "Summary Final Report. The Computerized Anatomical Man (CAM) Model". Report MDC G-4655, McDonnell-Douglas Corp., Huntington Beach, CA, 1973.
7. Yucker, W. R. and Huston, S. L.: "Computerized Anatomical Female. Final Report". Report MDC H-6107, McDonnell-Douglas Corp., Huntington Beach, CA, 1990.
8. Anon.: "1990 Recommendations of the International Commission on Radiological Protection." ICRP Publication 60, Pergamon Press, Inc., 1991.

9. Katz, R.; Zachariah, R.; Cucinotta, F. A.; and Zhang, C.: "Survey of Cellular Radiosensitivity Parameters". Radiation Research, **140**, pp. 356,365, 1994.
10. Cucinotta, F. A.; Katz, R.; Wilson, J. W.; and Dubey, R. R.: "Heavy Ion Track Structure Calculations for Radial Dose in Arbitrary Materials". NASA TM-3497, 1995.
11. Katz, R.; Cucinotta, F. A.; Wilson, J. W.; Shinn, J. L.; and Ngo, D, M.: "Track Structure Model of Cell Damage in Space Flight". NASA TP-3235, 1992.
12. Goodhead, D. T.: "Relationships of Radiation Track Structure to Biological Effect: A Re-interpretation of the Parameters of the Katz Model". Nucl. Tracks and Radiation Meas., **16**, no. 2/3, pp. 177-184, 1989.